

2,6-Bis(E)-4-Methylbenzylidene)-Cyclohexan-1-One As A Fluorescent-On Sensor For Ultra-Selective Detection Of Chromium Ion In Aqueous Media

Maria Sadia (✉ mariasadia@gmail.com)

University of Malakand <https://orcid.org/0000-0003-0818-170X>

Jehangir Khan

University of Malakand

Syed Wadood Ali Shah

University of Malakand

Robina Naz

University of Malakand

Faiz Ali

University of Malakand

Research Article

Keywords: Fluorescent-on sensor, chromium, aqueous samples, sensing

Posted Date: July 7th, 2021

DOI: <https://doi.org/10.21203/rs.3.rs-560875/v1>

License:   This work is licensed under a Creative Commons Attribution 4.0 International License.

[Read Full License](#)

Abstract

In current decade, curcumin and its analogues have been broadly used in biological field. However, there are relatively fewer studies regarding their fluorescence based applications for chromium ion sensing in water samples. This article, hereby, reports the synthesis, FTIR and $^1\text{H-NMR}$ spectroscopic analyses and optical description of 2,6-bis(E)-4-methylbenzylidene)-cyclohexan-1-one (sensor C), as a fluorescence-on sensor for trace level sensing of chromium. The sensor C exhibited an ultra-selective response to chromium among the tested heavy metal ions. Different parameters were optimized like pH, effect of concentration of sensor C, metal ion and contact time. The binding stoichiometry of C : Cr^{3+} was calculated to be 2:1 (Job's plot) with a significantly low detection limit of 2.3×10^{-9} M. Sensor C were practically employed for detection of chromium in spiked water samples.

Introduction

Chromium is considered one of the major toxicant due to its high solubility and mobility in water. Most of the pollutants in environment are degraded gradually by living organisms into simpler harmless substances; but some pollutants including heavy metal ions like chromium are non-degradable [1, 2]. Chromium is mainly added to water bodies either from natural sources; like volcanic eruption, rock weathering or man-made activities; including mining operations, metal extraction, production of alloys, steel industries, and pigment producing factories, improper waste disposal, electroplating, synthetic fertilizers and other fields. In environment chromium readily gets dissolved in water and is persistent for longer period of time within the bodies of organisms [3, 4], causing a number of disorders in organisms like tumors, gastrointestinal infections, ulceration, dermal irritation, lung cancer and anemia.

Several analytical methods such as absorption spectrometry [5], plasma mass spectroscopy [6], chemical reduction [7], adsorption [8], electrocoagulation [9], chemical precipitation [10], flotation [11], ion exchange [12], electrochemical [13] and amperometric analysis [14] have been applied for detection of chromium ions, but due to their time-consuming nature, complex operation, expensive instrumentations, sludge production, requirement of large amount of chemicals, and consequent risk of secondary pollutants, these techniques are not preferred for the trace detection of chromium. In the last few years, the development of optical sensors capable of sensing heavy metal ions is greatly demanded.

Among the metal ion sensors, fluorescence sensors have gained attention, since they contribute high sensitivity, lower cost, able to respond quickly, easily availability, excellent photo-physical properties, wide use, subsequent impact on the environment and nature, the easy operability, possibility of real time monitoring [15] and technological simplicity. The process of fluorescence based sensing is that upon light emission by fluorophore as soon as excited [16].

A number of fluorescent sensors have already been reported and were efficient employed for selective metal ion recognition and studies of these fluorescent probes yielded promising results in terms of specificity [17, 18].

The design and synthesis of fluorescence based receptors for their applications for chromium ion detection in environmental samples is still demanding research topic, as the determination of chromium by spectrofluorimetry is rarely studied [19].

Curcumin has very exciting photo physical and fluorescence properties. Apart from their application in biological field, the chemically synthesized pi-extended derivatives of curcumin analogues, possessing variety of chemical sites can be used as a potential sensor for metal ion determination. In current study, we report the development of curcumin derivative as a potential fluorochrome possessing efficient optical properties and binding capability. Due to the presence of electron donor atoms in the chemical structure of curcumin, it can easily form stable complex with cations [20].

Material And Methods

Required Materials

All the chemicals and reagents used in the current study were used as received. Cyclohexanone (Merck) 4-methylbenzaldehyde (Sigma Aldrich), sodium hydroxide (Alfa Aesar), methanol (Sigma Aldrich), Acetonitrile (Merck). Quartz cuvette was used for fluorometric chromium ion determination. All salts, in the form of sulphate, hydroxide and chloride form including $\text{Cd}(\text{SO}_4)_2 \cdot 4\text{H}_2\text{O}$, $\text{Ca}(\text{OH}_3)_2 \cdot 4\text{H}_2\text{O}$, $\text{Co}(\text{OH}_3) \cdot 6\text{H}_2\text{O}$, $\text{Zn}(\text{SO}_4)_2 \cdot 6\text{H}_2\text{O}$, $\text{Cu}(\text{SO}_4)_2 \cdot 3\text{H}_2\text{O}$, $\text{Mn}(\text{OH}_3)_2 \cdot 4\text{H}_2\text{O}$, and $\text{Ni}(\text{SO}_4)_3 \cdot 6\text{H}_2\text{O}$, $\text{CrCl}_3 \cdot 6\text{H}_2\text{O}$ were purchased from BDH chemical England.

Instrumentation

Fluorescence analyses were performed with spectrofluorophotometer RF-5301PC (Shimadzu, Japan). Ultraviolet-Visible spectroscopic analysis was accomplished with double-beam UV-Visible spectrophotometer (Shimadzu, Japan) model 1601. For $^1\text{H-NMR}$ and IR spectra characterization Bruker Advance 400 MHz spectrometer and FTIR spectrophotometer Pretige 21 (Shimadzu, Japan) was used respectively.

Solutions preparation for Spectroscopic measurements

Stock solution of sensor C in acetonitrile, and metal ions solutions using respective salts of nickel, cadmium, lead, cerium, copper, mercury, zinc, and manganese and chromium were prepared in distilled water. Working solutions were prepared from stock solution by appropriate dilution.

Sensor C synthesis and characterization

The sensor C [2,6-bis(E)-4-methylbenzylidene)-cyclohexan-1-one] was synthesized with slight modification of already existing method in literature [21] by reacting aldehyde and ketone in specific ration i.e. 2: 1. To a 12 mmol 4-methyl benzaldehyde (0.26 g in 12 mL ethanol) was added 6 mmol of cyclohexanone with continuous addition of sodium hydroxide (40 %). The resulted mixture was refluxed for 4 hours and the progress of reaction was observed using TLC. The product formed was processed in ice to get the final

products. Yellow colored pure crystals formed having melting point of 159°C (yield 78 %) and is given in (scheme 1). ¹H NMR: δ 7.78 (s, 2H, =CH), 7.46 (d, 4H, ArH), 6.94 (d, 4H, ArH), 3.86 (s, 6H, 2CH₃), 2.92 (dd, 4H, J = 14.6, 2.7 Hz), 1.82 (m, 2H, CH₂) (Fig. S1) [22]. The IR (KBr) spectrum (ν cm⁻¹): 1626–1642 (C = C Ar), 3000 – 2930 (C-H asymmetric), 1710 (C = O) 3030, (C-H Ar) (Fig. S2) [23].

Spectroscopic studies

For exploring optical properties and sensing capability of sensor C for chromium detection UV-Vis and fluorescence spectrometry were used. The fluorescence and absorption spectra were taken in acetonitrile due to its freely solubility in it. In all of the spectroscopic experiments distilled water was used for metal solution and their spectra were recorded accordingly. For Uv/vis analysis, test solutions containing a fixed amount (8 μM) of sensor C while chromium (2–12 μM) concentration range were mixed and recorded. The fluorescence response of sensor C was monitored before and after mixing with different metal ions in distilled water. The mixtures were equilibrated at room temperature before measuring the fluorescence response. In addition, the practical applicability of sensor C for chromium ion determination in the vicinity of co-existing of similar metal cations in aqueous media was also investigated.

Quantum yield calculation

Rhodamine 6G dye was used as a standard possessing quantum yield (φ) 95 % for enumerating quantum yield of the sensor C. For doing the experiment, Rhodamine 6G solution was prepared and its spectroscopic analysis (UV-Visible absorption and fluorescence) were performed. The quantum yield was determined with the help of the given formula

$$\varphi_C = \varphi_R \left(\frac{I_C}{I_R} \right) \left(\frac{\eta_C^2}{\eta_R^2} \right) \left(\frac{A_R}{A_C} \right) \quad (1)$$

Where “C” and “R” represent sensor C and dye respectively. “I” represent the integrated fluorescence intensity, “η” correspond to refractive index of solvent and “A” correspond to absorbance.

Analytical sensitivity

Stern Volmer plot analysis were performed for detection limit (δ) and quantification limit (β) determination using Eqs. 2 and 3 respectively

$$LOD = \frac{3\delta}{S} \quad (2)$$

$$\beta = \frac{10\delta}{S} \quad (3)$$

Where represent the standard deviation, and S being the slope of fluorescence response versus concentration curve. The respective experiment was performed seven times to examine the replicability of the system.

Computation of binding constant

To calculate approximately the binding constant of sensor C (Benesi-Hilderbrand plot) was drawn between fluorescence intensity and reciprocal of chromium concentration. The binding constant was attained using the given Eq. 4.

$$\text{Binding constant}(B.C) = \frac{\text{Intercept}}{\text{Slope}} \quad (4)$$

Spiking of natural water samples

Fluorescence spectroscopy was used for detecting the ability of the sensor C towards the ion of interest, Chromium, in real water samples. Therefore, the selected water samples (river water, Tap water) were used for spiking of different concentration of chromium (2–12) μM in the presence of (8 μM) sensor C and the fluorescence response was measured at specific wavelengths of excitation and emission. For verification of the test results, all analysis were four times repeated.

Results And Discussion

Ultraviolet-Visible study

For the evaluation of the photophysical properties of sensor C and its chromium complex UV-Visible analysis was initially used. For considerable solubility and prospective applicability of sensor C, acetonitrile was selected as a solvent for sensor C in the current study. Ultraviolet-Visible spectrum of sensor C was taken in the presence and absence of different concentration of chromium ions. The Uv/vis spectrum for sensor C showed characteristic main absorption band (λ_{max}) at 360 nm. Upon addition of chromium solution bathochromic shift occurred and maximum absorption band appeared at 420nm, confirming the formation of chromium complex with sensor C (Fig. 1). Each time baseline was established by putting respective blanks in the reference slot.

Cation sensing studies using fluorescence spectroscopy

Fluorescence-on studies by Cr^{3+} ion

In our ongoing detection for a better understanding and a feasible intonation of the sensing ability of curcumin based fluorochrome, we have tagged curcumin based sensor with metal ion. In order to realize the photo physical properties of sensor C prior to metal ions recognition, the fluorescence response of free sensor C was taken. According to results obtained, sensor C displayed a very weak emission peak at 560 nm (λ_{em}). To investigate metal ion sensing by sensor C, different heavy metal ions Ni^{2+} , Ce^{3+} , Cu^{2+} , Zn^{2+} , Cd^{2+} , Mn^{2+} , Cr^{3+} , Pb^{2+} , Co^{2+} (200 μM) were added to sensor C solution separately. The respective mixtures were allowed for 3 minutes to equilibrated, and were transferred into quartz cuvette separately by monitoring fluorescence intensity in the range of 400–700 nm. The spectra obtained for all the studied metal was compared with the spectrum of sensor C. Accidentally, in our case, a prominent enhancement in fluorescence emission intensity was observed at λ_{em} 560 nm upon the addition of aqueous chromium ion (200 μM) to sensor C solution. While no apparent enhancement in intensity was spotted for the rest of

metal ions (Fig. 2). So among the studied metal ions only chromium form complex with sensor C. This specific fluorescence-on response could be accredited to restriction of ICT phenomena. In the absence of chromium ions, due to ICT phenomena, a weak fluorescence was observed for sensor C. while in the presence of chromium ions ICT process is negligible and fluorescence intensity was extensively enhanced as the result of formation of a stable complex [24].

As discussed, we postulated that the apparent fluorescence enhancement of sensor C could be ascribed to a distinctive chemical resemblance for chromium ion. It is presented in already reported articles, fluorescent molecules like sensor C retain certain preference for chromium ion, thus allow a superficial prejudice from its close neighbor Fe^{3+} along with other similar co-existing ions through fluorescence enhancement [25].

pH study

In the interests of avoiding interference in chromium ion recognition by protons, we focused on pH analysis on the fluorescence retaliation. The pH value of the test system was set to acquired value by HCl and NaOH solution. The sensor C ($8 \mu\text{M}$) did not change its fluorescent intensity from pH = 1 to 14, indicating its consistency. The weak fluorescent response of sensor C may be owing to intra-molecular photo-induced electron transfer. However, sensor C complex with ($16 \mu\text{M}$) chromium showed strong fluorescence at pH 8, on account of its binding with Cr^{3+} leading to intra-molecular photo-induced electron transfer process inhibition. The chromium complex was unstable at lower pH thus displaying quenching in intensity as a result of protonation carbonyl oxygen that acts as binding site. By gradually increasing the pH, the fluorescence intensity strikingly enhanced (Fig. 3). At pH 8, high stability was displayed by the chromium complex and maximum enhancement in intensity was observed at λ_{em} 560 nm. While at pH > 8, a gradual decrease in intensity occurred due to formation of hydroxyl complexes that had poor solubility in water solution. From the results obtained, it can be assumed that the synthesized sensor C can successfully be used for chromium ion determination at pH 8 in aqueous samples [26].

Sensor C concentration effect

The determination of concentration effect of sensor C on fluorescence response of the sensor C- Cr^{3+} complex is one of the important parameters in fluorimetric analyses. Working solution for analysis were prepared by keeping the chromium concentration constant ($16 \mu\text{M}$), and varying the sensor C concentration in the range of 5–40 μM . The fluorescence emission intensity of each sample was monitored in 440–700 nm range (Fig. 4). With increasing concentration of sensor C, a linear enhancement in the emission intensity was observed. At higher concentration, the fluorescence intensity remains constant.

Quantitative study for Cr^{3+}

For the confirmation of sensitivity of sensor C toward chromium ion, fluorescence titration experiments were carried out. During these titrations, the sensor C concentration was kept constant while changing the

chromium ions concentration from 1–15 μM . A linear enhancement in the fluorescence intensity of chromium complex was noted at 560 nm (λ_{em}) upon increasing chromium concentration (Fig. 5). Thus showing that sensor C can be used for quantitative determination of Cr^{3+} .

Binding mode study

The binding stoichiometry between sensor C and chromium was investigated using a Job's plot, A Job's plot between the different mole fraction of sensor C- Cr^{3+} complex versus respective emission intensities showed a maxima at 0.7 mole fraction indicating a 2:1 stoichiometric ratio between sensor C and Cr^{3+} (Fig. 6).

This 2:1 binding ratio was further confirmed with the help of Benesi-Helderbrand plot. For this purpose, for determination of association constant the given equation was used

$$\frac{F_{\text{max}} - F_0}{F - F_0} = 1 + \frac{1}{K [\text{Cr}^{3+}]^2} \quad (5)$$

Where K (M^{-2}) represent association constant. F_0 , F_{max} and F denote the emission intensity of free sensor C, at $[\text{Cr}^{3+}]$ in excess concentration and at different $[\text{Cr}^{3+}]$ ($\lambda_{\text{ex}} = 425$ nm and $\lambda_{\text{em}} = 560$ nm) respectively. The value of K was determined by plotting $F_{\text{max}} - F_0 / F - F_0$ versus $1/[\text{Cr}^{3+}]^2$, (Fig. 7). According to the Equation, data fitted linearly, showing good liner relationship with slope 6.515×10^{-11} , and intercept 1.539. The association constant calculated from the slope is found to be 1.53×10^{10} thus confirming the 2:1 binding ratio between sensor C and Cr^{3+} .

The detecting mechanism of fluorescent sensor C for Cr^{3+}

The detecting mechanism of sensor C for Cr^{3+} ion was suggested using the fluorescence spectra. The fluorescent response of the sensor C towards Cr^{3+} ion may be allocated to intra molecular charge transfer (ICT). Before being coordinated with Cr^{3+} ions, sensor C displays a weak fluorescence emission spectrum due to lone electron pair of oxygen atom, which result in intra molecular charge transfer. Moreover, the lone electron pair of the oxygen atom give rise to a non-radiative process by the $n-\pi^*$ transition, as a result quenching in fluorescence intensity takes place. On the other hand, after sensor C was coordinated to Cr^{3+} ion, radiation process was primarily via $\pi-\pi^*$ transitions and the coordination complex was more rigid thus the ICT process was restricted upon addition of Cr^{3+} ion at the receptor site.

On the other hand, sensor C act as monodentate ligand as there is one potential coordination cite, the carbonyl oxygen. The coordination sphere of d-block elements like Cr is either 6 or 2 and complexes of chromium with both these coordination spheres have been reported [27–30]. Since the bulk of our sensor C is high so the bonding with chromium is expected to be strong and possible structures of sensor C- Cr^{3+} complex have been proposed in the (Scheme 2).

Table 1
Photophysical properties of sensor C

Parameter	C:Cr ³⁺	$\lambda_{em}(nm)$	$\lambda_{ex}(nm)$	LOD (Cr ³⁺)	Quantum yield (%)
Sensor C	2: 1	560	425	2.3×10^{-9} M	72

Time study

Rapid response time is highly preferred in fluorimetric studies, therefore the time effect on emission response of sensor C and its complex with chromium was studied in time range of 0–7 min for different concentrations of chromium. During the assay, the fluorescence emission response of sensor C remained unaffected with increasing time, whereas the complex showed a linear response in fluorescence intensity with time and maximum fluorescence response was observed at 2 min and then remained constant (Fig. 8). These results indicate effectivity of sensor C for real time assay of chromium detection in environmental samples.

Effect of competitive metal cations

Competitive binding experiments were taken for evaluation of efficacy of the synthesized sensor C as a selective chromium ion sensor as sensor C should have the potential to detect chromium ions in the presence of co-existing metal cations. For this purpose, different commonly existing metal ions in water were selected like Cu²⁺, Hg²⁺, Zn²⁺, Cd²⁺, Pb²⁺, Mn²⁺, Co²⁺, Ni²⁺ including the closely related ions like Ce³⁺. The concentration of each interfering metal ion was taken 8 folds (128 μM) as compared to chromium metal ion (16 μM) while keeping the sensor C concentration constant (8 μM). The fluorescence emission profiling was completed between 440–700 nm with 425 nm λ_{ex} .

No interference in fluorescence results in terms of intensity occurred even in the presence of high concentrations of interfering ions (Fig. 9). Thus, the obtained results may indisputably provide the reported sensor C is particularly valuable in efficiently selective chromium ion determination from its chemically similar cations like cerium and other commonly found interfering ions. Therefore, it can be realistically incidental that the synthesized sensor C exhibits an ultra-sensitive and highly selective fluorescence-on response toward chromium ion in aqueous samples.

Reversibility of sensor C

To determine whether the metal complex formation process is reversible or not, fluorescence emission titration experiment was performed using the sensor-Cr³⁺ complex with EDTA.

The reversibility of the designed fluorescence-based sensor is curricula for its economy and many times usage. In this regard, EDTA is added into sensor C combined with Cr³⁺ solution to confirm the effect of Cr³⁺ ions on the fluorescence response. When EDTA is added to the aqueous solution, the fluorescence spectrum is returned to its original state. The interaction between sensor C and Cr³⁺ ions is prevented by the formation of Cr³⁺-EDTA chelate. After the addition of EDTA, the fluorescence of sensor C is

recovered. The fluorescence-on sensor C is proved to be reversible using turn off–on mechanism based on the fluorescence emission intensity measurement (Fig. 10). The experiments were repeated 4 times by getting the same results. Furthermore, since the fluorescence emission intensity was restored upon addition of EDTA, the sensing process was considered to be reversible rather than an ion-catalyzed reaction.

Quantitative detection of Cr ion in aqueous samples

To study in deep the suitability and on-field applicability of prepared sensor C for ultra-selective detection of chromium ion, the different water samples were spiked by adding chromium to have sample solutions in (1–10) μM conc. range. Accordingly, the results attained displayed a significant recovery of chromium ions from different environmental water samples (Fig. 11). Thus, we presented a cost efficient method for highly selective determination of Cr^{3+} ion in aqueous samples.

Significance of Current Work

As compared to other chromium ion detection methods (Table 2), the present methodology has the compensation in terms of linearity and ultra-low sensitivity. In addition, it display higher potential for chromium detection.

Table 2
Comparison of some sensors for chromium ions determination

Sensors	Limit of detection	Fluorescence response	Analyte	Optimal pH	Testing media	Ref
5,5'-bipyridyl-Idicarboxaldehyde	NA	turn-on	Cr ³⁺	6	Aqueous	[31]
carbon quantum dots	0.64×10^{-6} M	turn-off	Cr ³⁺	8	Aqueous	[32]
5-((2-cyano-[1,1-biphenyl]-4-yl)-methoxy)isophthalic acid	1.4×10^{-6} M	turn off	Cr ³⁺	8	Aqueous	[33]
rhodamine B lactams	1×10^{-7} M	turn on	Cr ³⁺	7	NA	[34]
asparagine derivatives	1.6×10^{-8} M	turn on	Cr ³⁺	7	NA	[35]
curcumin derivative	2.3×10^{-9} M	turn-on	Cr ³⁺	8	Aqueous	Current work

Conclusion

In summary, we have developed a sensor C for a possible Cr³⁺ ion-selective detection in aqueous samples. The sensor C exhibited remarkable sensing properties in terms of fluorescence response, sensitivity, selectivity and detection limit. Specially, sensor C showed a highly selective response for chromium among other interfering metal ions with limit of detection and limit of quantification 2.3×10^{-9} M and 3.14×10^{-8} M respectively. Considering the photo-physical properties and the chemosensing capability, the highly emissive curcumin-based sensor C, [2,6-bis(E)-4-methylbenzylidene)-cyclohexan-1-one] can be considered as one of the very promising candidate for chemosensing applications. Validity of the present method was effectively realized by real sample assay.

Declarations

Declaration of interest

The authors declare no competing financial interest.

Acknowledgements

We thank Department of Chemistry, University of Malakand for providing chemicals and research lab facility for conduction of the present work. We also extend our appreciation to Prof. Dr. Yuta Nishina and Dr. Rizwan Khan (Research Core for Interdisciplinary Sciences, Okayama University, Japan) for their help in characterization of the synthesized compounds.

Supplementary data

FTIR and $^1\text{H-NMR}$ spectra of sensor C, fluorescence emission profile as a function of Cr^{3+} ion, time course of the fluorescence response, titration curve from absorption analysis the response of sensor C towards Cr^{3+} , titration curve of sensor S- Cr^{3+} complex, Jobs plot analysis, effect of Cr^{3+} ion concentration, Benesi-Hilderbrand plot, reversibility, pH study. Supplementary data to this article can be found online.

Author Declarations

Funding

There has been no significant financial support for conduction of current research work that could have influenced its outcomes.

Conflicts of interest

The authors declare that they have no conflicts of interest.

Ethics declarations

In the current study the procedure adopted is safe both for animals, humans and their environment.

Consent to participate

All the authors are consent to participated in the current research work. Consent for publication All the authors have given their consent of publishing this article in the said journal.

Authors' contributions

Jehangir Khan

Carried out the main experimental work.

Maria Sadia

Encouraged, supervised the findings of the work and took the lead in writing the manuscript.

Syed Wadood Ali Shah

Supervised the project, conceived and planned the experiments.

Robina Naz

Contributed to the interpretation of the results.

Faiz Ali

Contributed to the final version of the manuscript.

All authors provided critical feedback and helped shape the research, analysis and manuscript.

Data Availability

All the data associated with this research has been presented in this paper.

References

1. Filice FP, Henderson JD, Li MS, Ding Z (2019) Correlating live cell viability with membrane permeability disruption induced by trivalent chromium. *ACS omega* 4(1):2142–2151
2. Bieber VS, Ozcelik E, Cox HJ, Ottley CJ, Ratan JK, Karaman M, Badyal S (2020) Capture and release recyclable dimethylaminomethyl-calixarene functional cloths for point-of-use removal of highly toxic chromium water pollutants. *ACS Appl Mater Interfaces* 12(46):52136–52145
3. Vellaichamy B, Periakaruppan P, Nagulan B (2017) Reduction of Cr⁶⁺ from wastewater using a novel in situ-synthesized PANI/MnO₂/TiO₂ nanocomposite: renewable, selective, stable, and synergistic catalysis *ACS Sustain. Chem Eng* 5(10):9313–9324
4. Barbosa RF, Souza AG, Maltez HF, Rosa DS (2020) Chromium removal from contaminated wastewaters using biodegradable membranes containing cellulose nanostructures. *Chem Eng J* 395:125–135
5. Suo L, Dong X, Gao X, Huang JX, Ye J, Zhao L (2019) Silica-coated magnetic graphene oxide nanocomposite based magnetic solid phase extraction of trace amounts of heavy metals in water samples prior to determination by inductively coupled plasma mass spectrometry. *Microchem J* 149:104–112
6. Lei C, Wang C, Chen W, He M, Huang B (2020) Polyaniline magnetic chitosan nanomaterials for highly efficient simultaneous adsorption and in-situ chemical reduction of hexavalent chromium: removal efficacy and mechanisms. *Sci Total Environ* 733:139–146
7. Ding J, Pu L, Wang Y, Wu B, Yu A, Zhang G, Gao X (2018) Adsorption and reduction of Cr (VI) together with Cr (III) sequestration by polyaniline confined in pores of polystyrene beads. *Environ Sci Technol* 52(21):12602–12611

8. Khan SU, Islam DT, Farooqi IH, Ayub S, Basheer F (2019) Hexavalent chromium removal in an electrocoagulation column reactor: Process optimization using CCD, adsorption kinetics and pH modulated sludge formation. *Process Saf Environ Prot* 122:118–130
9. Kim T, Kim TK, Zoh KD (2020) Removal mechanism of heavy metal (Cu, Ni, Zn, and Cr) in the presence of cyanide during electrocoagulation using Fe and Al electrodes. *J Water Process Eng* 33:101–109
10. Mahdavi S, Jalali M, Afkhami A (2013) Heavy metals removal from aqueous solutions using TiO₂, MgO, and Al₂O₃ nanoparticles. *Chem Eng Commun* 200(3):448–470
11. Kołodyńska D, Bąk JK, Różańska JK, Pietrzak R (2017) Uptake of heavy metal ions from aqueous solutions by sorbents obtained from the spent ion exchange resins. *Microporous Mesoporous Mater* 244:127–136
12. Fu HR, Xu ZX, Zhang J (2015) water soluble metal-organic frameworks for fast and high dichromate trapping via single-crystal-single-crystal ion exchange. *Chem Mat* 27(1):205–210
13. Ouyang R, Bragg SA, chambers JQ (2012) Xue ZL Flower like self assembly of gold nanoparticles for high sensitive electrochemical detection of chromium (IV). *Anal Chim Acta* 722:1–7
14. Tumolo M, Ancona V, Paola DD, Losacco D, Campanale C, Massarelli C, Uricchio VF (2020) Chromium pollution in european water, sources, health risk, and remediation strategies: an overview. *Int J Environ Res Public Health* 17(15):54–68
15. Hao J, Li XY, Zhang Y, Dong WK (2018) A reversible bis(salomo)-based fluorescence sensor for selective detection of Cd²⁺ in water-containing systems and food samples. *Mater* 11(4):523–530
16. Acha ND, Elosua C, Corres JM, Arregui FJ (2019) Fluorescent sensors for the detection of heavy metal ions in aqueous media. *Sens* 19(3):599–604
17. Chu ZY, Wang WN, Zhang CY, Ruan J, Chen BJ, Xu HM, Qian HS (2019) Monitoring and removal of trace heavy metal ions via fluorescence resonance energy transfer mechanism: In case of silver ions. *Chem Eng J* 375:121–127
18. Chen S, Xue Z, Gao N, Yang X, Zang L (2020) Perylenediimide-based fluorescent and colorimetric sensors for environmental detection. *Sens* 20(3):917–923
19. Li E, Zeng X, Fan Y (2009) Removal of chromium ion (III) from aqueous solution by manganese oxide and microemulsion modified diatomite. *Desalination* 238(1–3):158–165
20. Prohl M, Schubert US, Weigand W, Gottschaldt M (2016) Metal complexes of curcumin and curcumin derivatives for molecular imaging and anticancer therapy. *Coord Chem Rev* 307:32–41
21. Carmona-Vargas CC, Alves DC, Brocksom TJ, Oliveira KT (2017) Combining batch and continuous flow setups in the end-to-end synthesis of naturally occurring curcuminoids. *React Chem Eng* 2(3):366–374
22. Badal MMR, Ashekul IHM, Maniruzzaman M, Abu Yousuf M (2020) Acidochromic behavior of dibenzylidene cyclohexanone-based bischalcone: experimental and theoretical study. *ACS omega* 5(36):22978–22983

23. Tamang N, Ramamoorthy G, Joshi M, Choudury AR, Kumar S, Golakoti NR, Doble M (2020) Diarylidene-cyclopentanone derivatives as potent anti-inflammatory and anticancer agents. *Med Chem Res* 29(9):1579–1589
24. Zhang H, Liu Q, Wang T, Yun Z, Li G, Liu J, Jiang G (2013) Facile preparation of glutathione-stabilized gold nanoclusters for selective determination of chromium (III) and chromium (VI) in environmental water samples. *Anal Chim Acta* 770:140–146
25. Dutta A, Mahapatra M, Deb M, Mitra M, Dutta S, Chattopadhyay PK, Singha NR (2020) Fluorescent terpolymers using two non-emissive monomers for Cr(III) sensors, removal, and bio-imaging. *ACS Biomater Sci Eng* 6(3):1397–1407
26. Saini A, Bhasin AK, Singh N, Kaur N (2016) Development of a Cr(III) ion selective fluorescence probe using organic nanoparticles and its real time applicability. *New J Chem* 40(1):278–284
27. Carney MJ, Robertson NJ, Halfen JA, Zakharov LN, Rheingold AL (2004) Octahedral chromium (III) complexes supported by bis (2-pyridylmethyl) amines: ligand influence on coordination geometry and ethylene polymerization activity. *Organometallics* 23(26):6184–6190
28. Doistau B, Collet G, Bolomey EA, Sadat-Noorbakhsh V, Besnard C, Piguet C (2018) Heteroleptic ter-bidentate Cr (III) complexes as tunable optical sensitizers. *Inorg Chem* 57(22):14362–14373
29. Al Thagfi J, Lavoie GG (2012) Synthesis, characterization, and ethylene polymerization studies of chromium, iron, and cobalt complexes containing 1, 3-Bis (imino)-N-heterocyclic carbene ligands. *Organometallics* 31(6):2463–2469
30. Park JE, Kang SK, Woo JO, Son KS (2015) Highly active chromium (III) complexes based on tridentate pyrazolyl pyridyl ligands for ethylene polymerization and oligomerization. *Dalton Trans* 44(21):9964–9969
31. Balamurugan G, Velmathi S (2018) Coplanarity driven fluorescence turn-on sensor for chromium (III) and its application for bio-imaging. *Photochem Photobiol Sci* 17(2):239–244
32. Feng S, Gao Z, Liu H, Huang J, Li X, Yang Y (2019) Feasibility of detection valence speciation of Cr (III) and Cr (VI) in environmental samples by spectrofluorimetric method with fluorescent carbon quantum dots. *Spectrochim Acta A Mol Biomol Spectrosc* 212:286–292
33. Sun Z, Yang M, Ma Y, Li L (2017) Multi-responsive luminescent sensors based on two-dimensional lanthanide–metal organic frameworks for highly selective and sensitive detection of Cr (III) and Cr (VI) ions and benzaldehyde. *Cryst Growth Des* 17(8):4326–4335
34. Zheng X, Zhang W, Mu L, Zeng X, Xue S, Tao Z, Yamatob T (2010) A novel rhodamine-based thiacalix [4] arene fluorescent sensor for Fe³⁺ and Cr³⁺. *J Incl Phenom Macrocycl Chem* 68(1):139–146
35. Esteves CI, Raposo MM, Costa SP (2011) Novel highly emissive non-proteinogenic amino acids: synthesis of 1, 3, 4-thiadiazolyl asparagines and evaluation as fluorimetric chemosensors for biologically relevant transition metal cations. *Amino Acids* 40(4):1065–1075

Figures

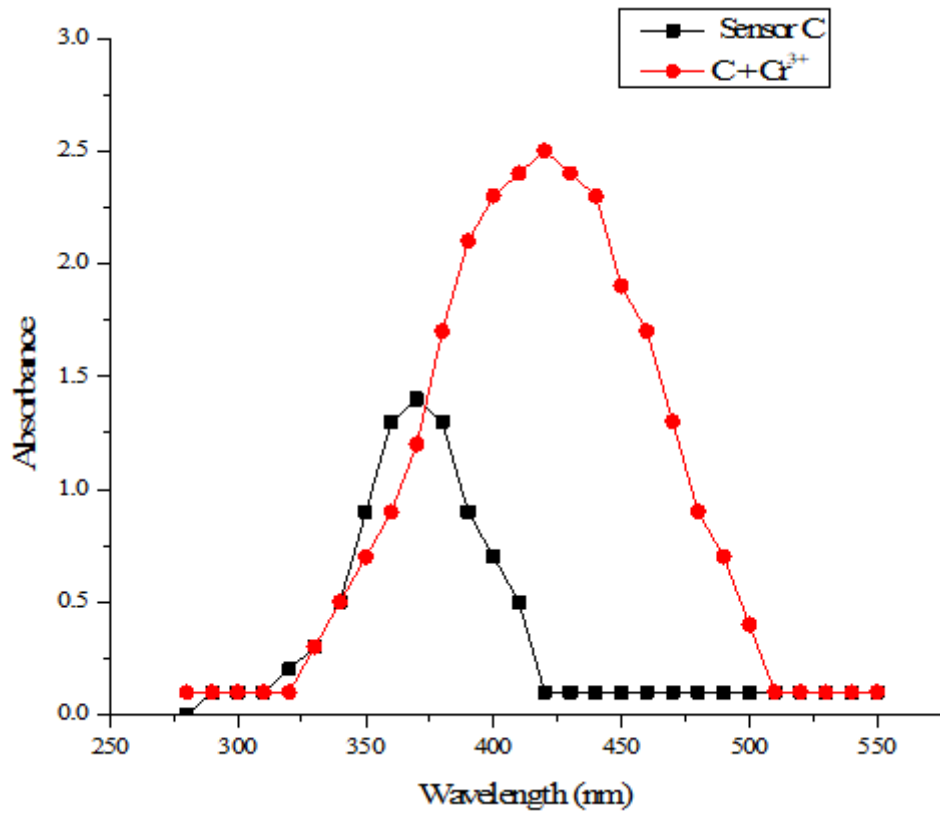


Figure 1

UV visible analysis of sensor C and its chromium complex

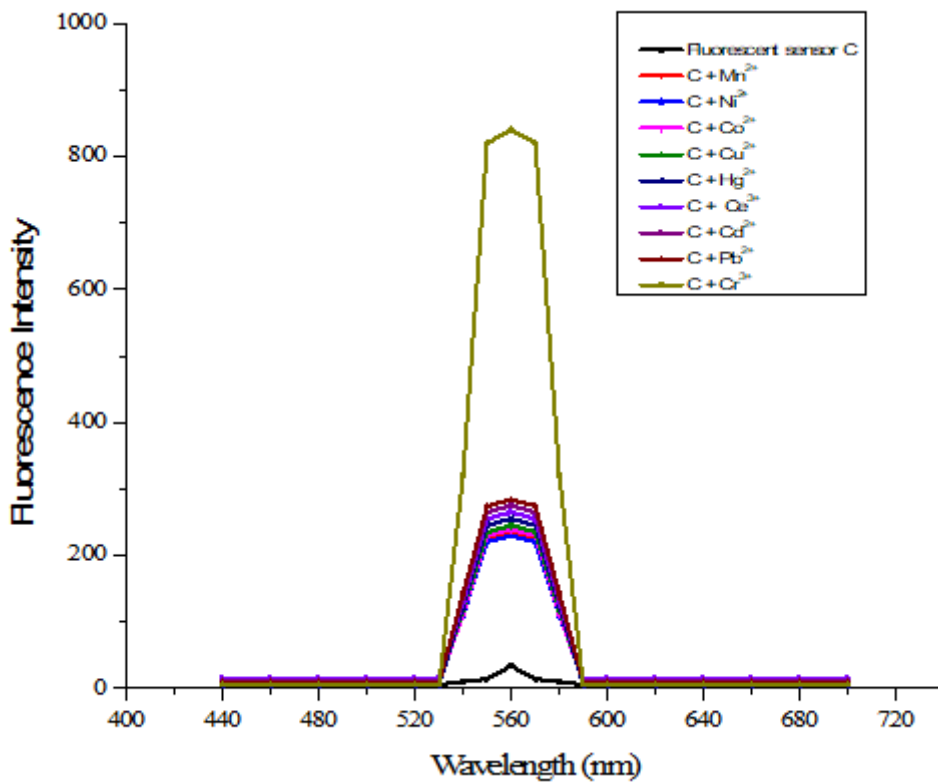


Figure 2

Fluorescence-on study of sensor C showing maximum fluorescence intensity at $\lambda_{em}560$ nm for chromium using sensor C, (8 μ M) and metal ions (200 μ M).

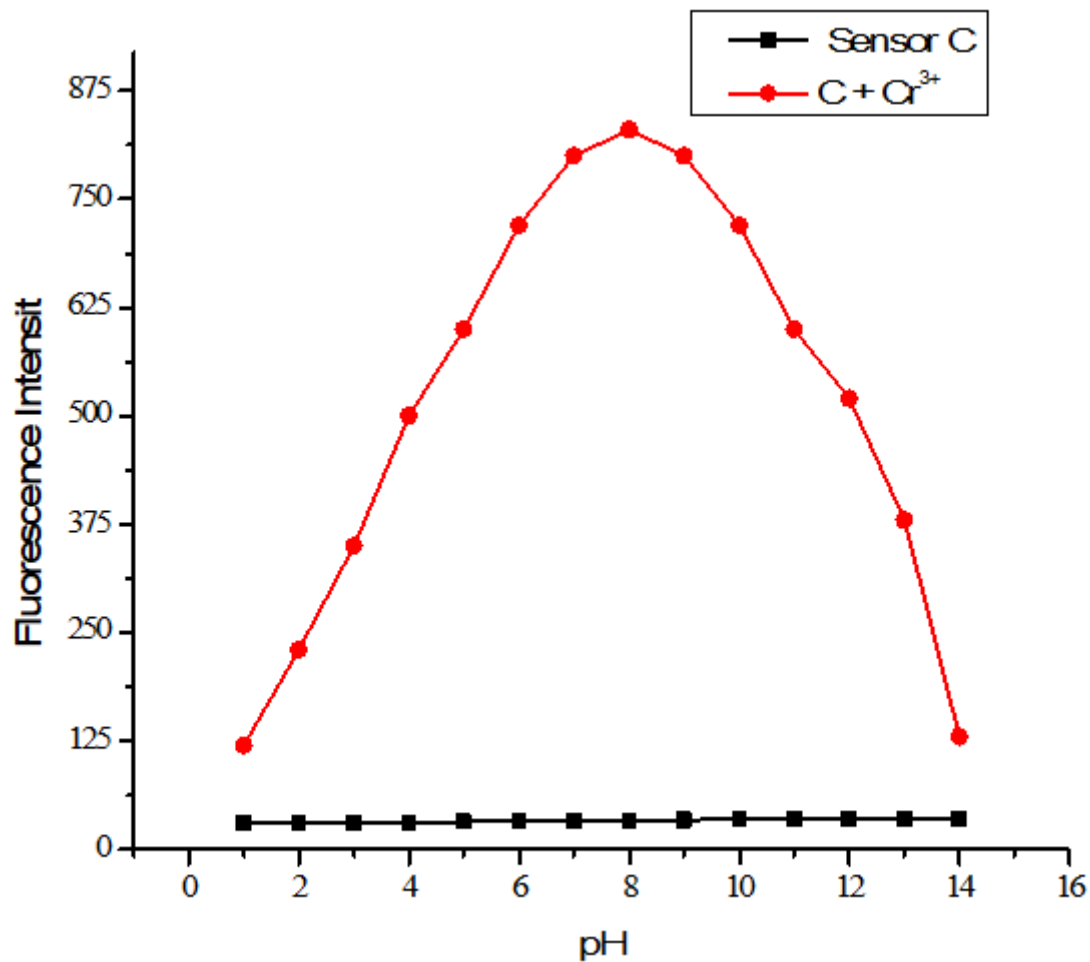


Figure 3

Changes in fluorescence emission intensity of sensor C and its complex with chromium with change in pH from 1-14 at wavelengths of emission 560 nm.

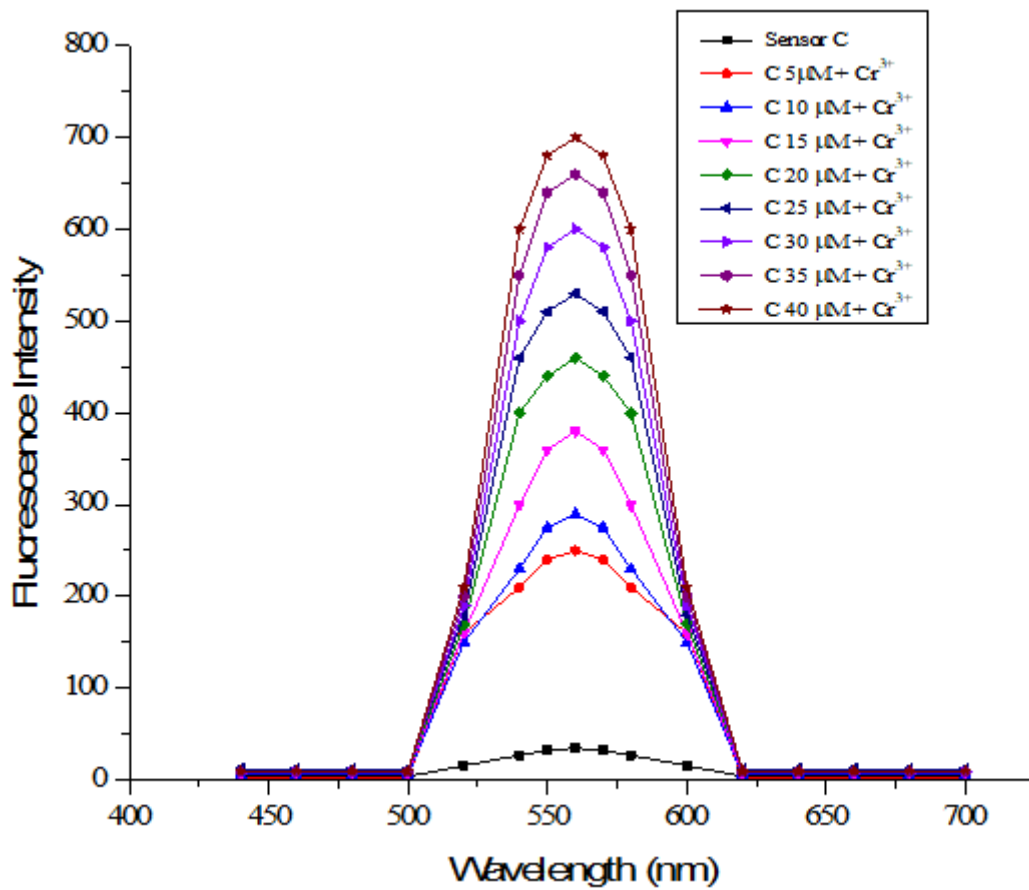


Figure 4

Fluorescence emission profile of sensor C-Cr³⁺ complex as a function of sensor C concentration (λ_{em} = 560 nm and λ_{ex} = 425 nm)

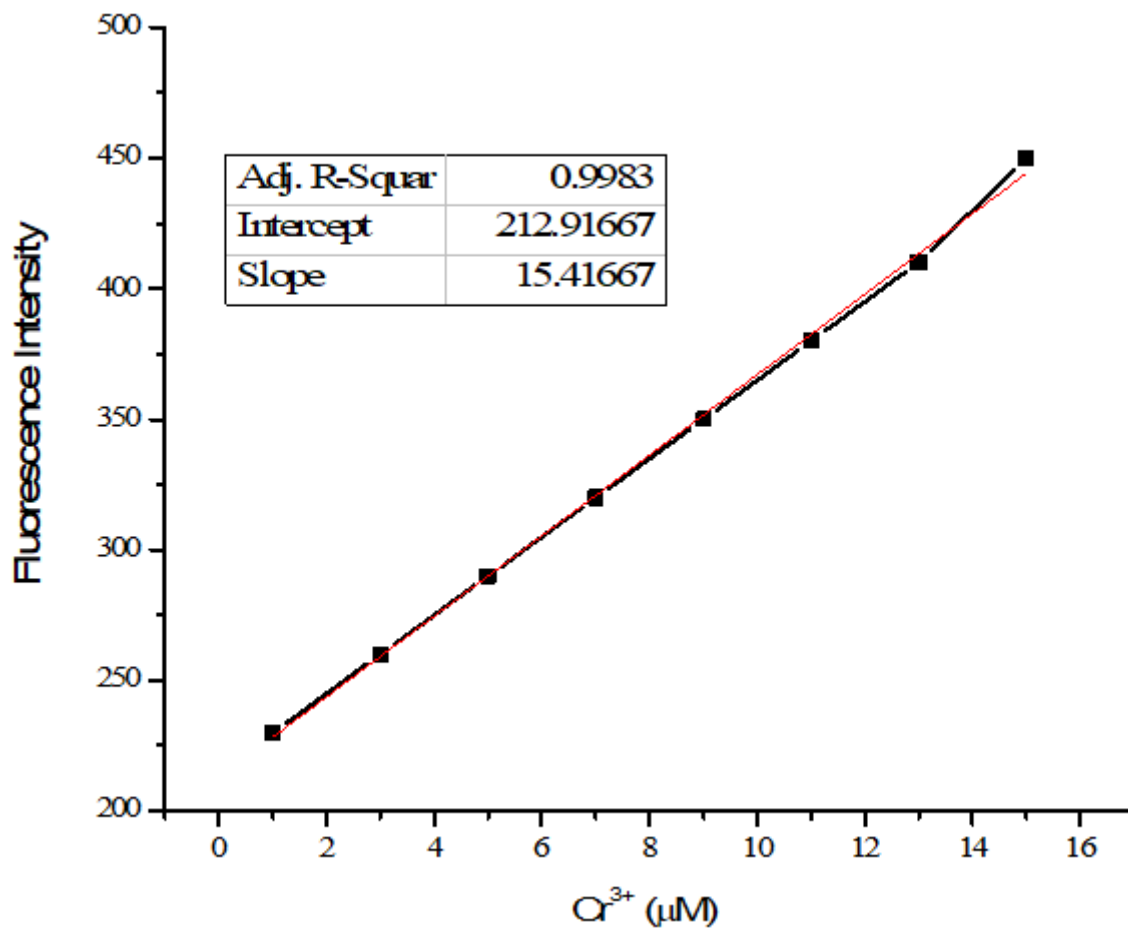


Figure 5

Fluorescence emission profile of sensor C-Cr³⁺ complex as a function of chromium ions concentration (λ_{em} = 560 nm and λ_{ex} = 425 nm).

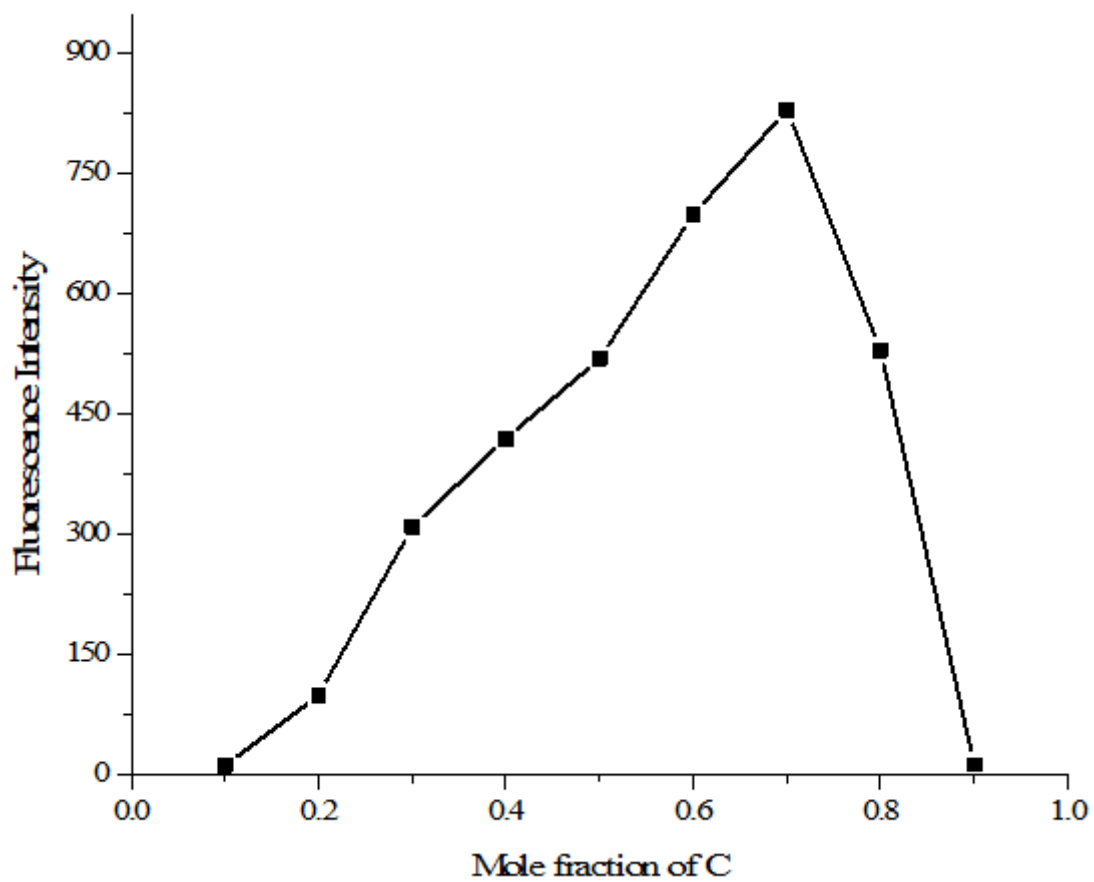


Figure 6

The job's plot examined between sensor C and Cr^{3+} , indicating the 2:1 stoichiometry, which was carried out by fluorescence spectra ($\lambda_{em} = 560 \text{ nm}$).

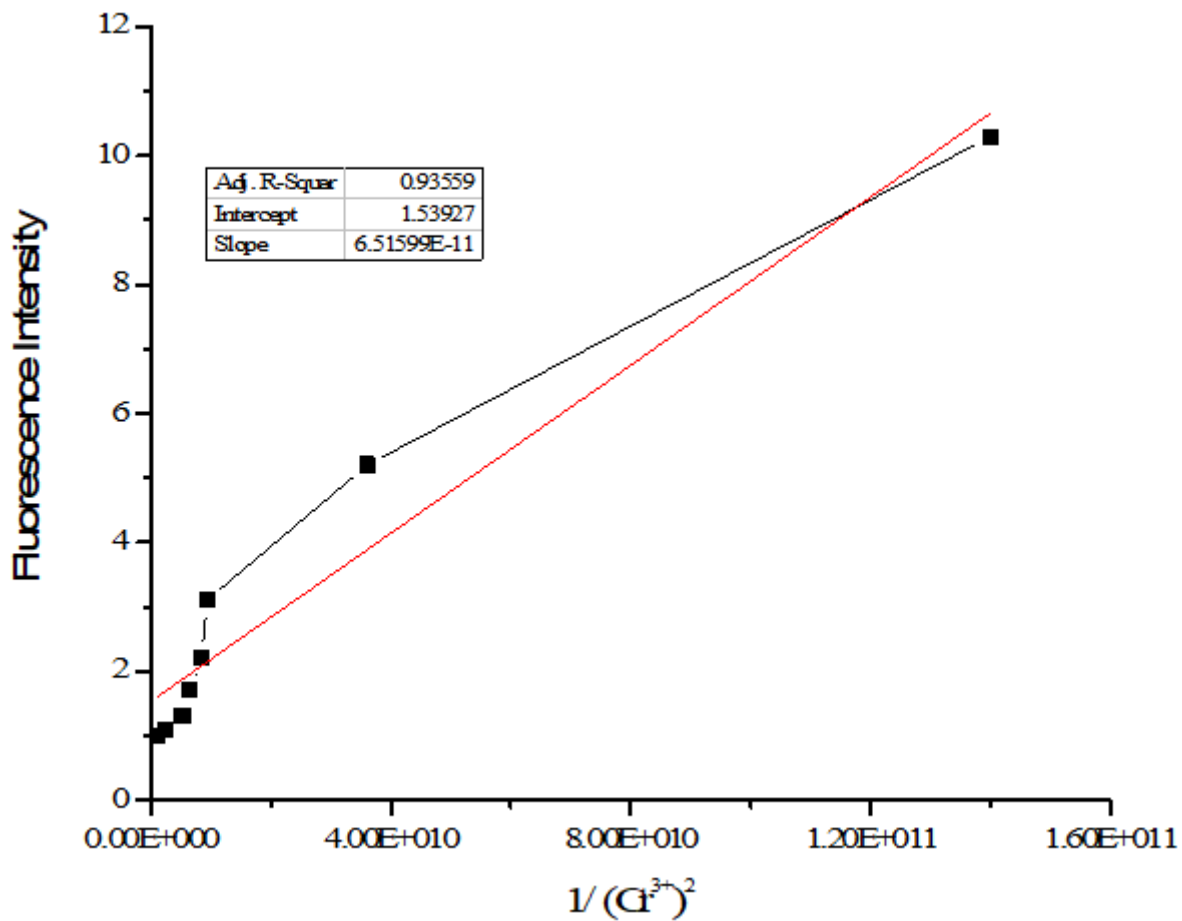


Figure 7

Bensi-Helderbrand Plot analysis for association constant determination

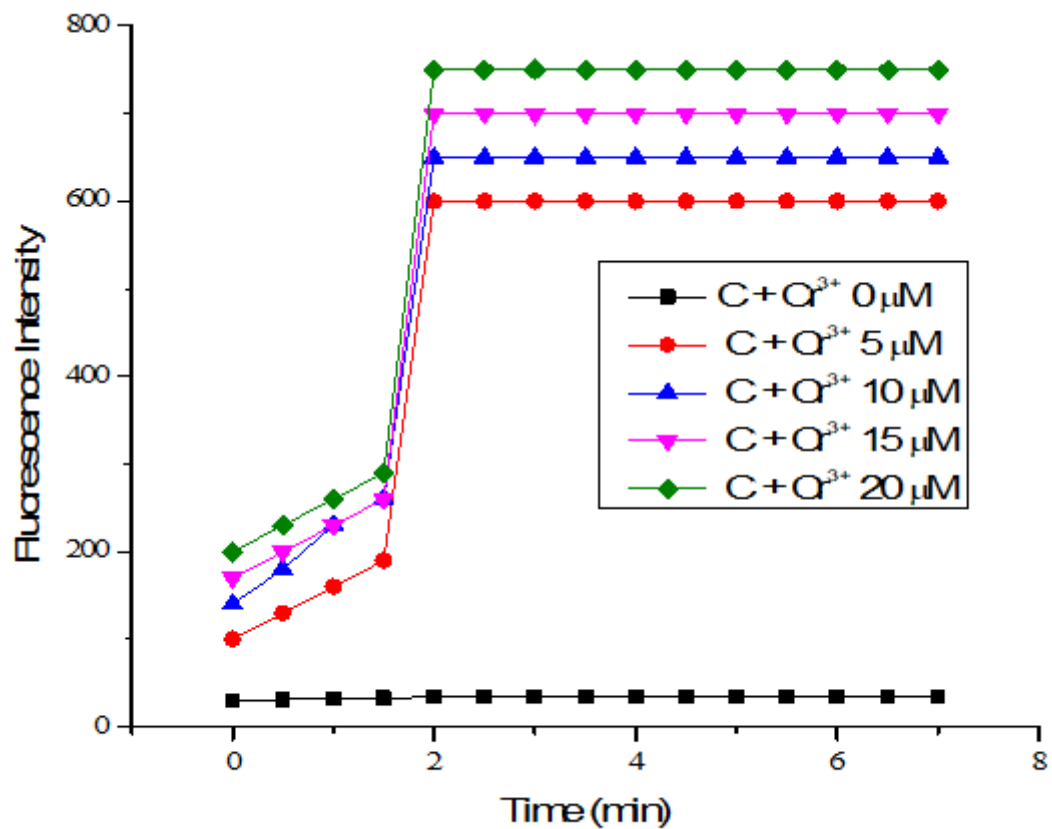


Figure 8

Effect of time on the fluorescence response of sensor C (8 μM) with chromium concentration in the range of (0-20 μM) at λ_{em}560 nm.

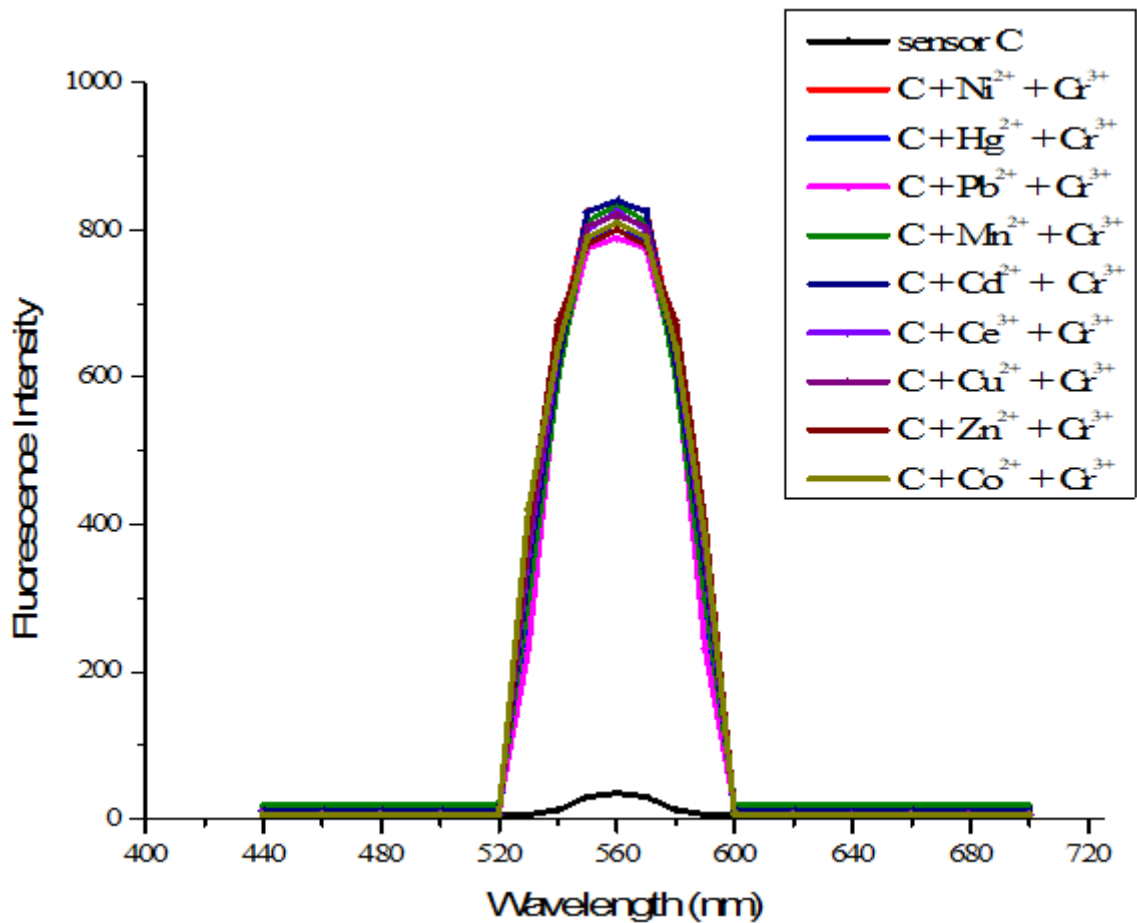


Figure 9

Selective response of sensor C for Cr³⁺ in the presence of interfering metal ions ($\lambda_{em} = 560 \text{ nm}$).

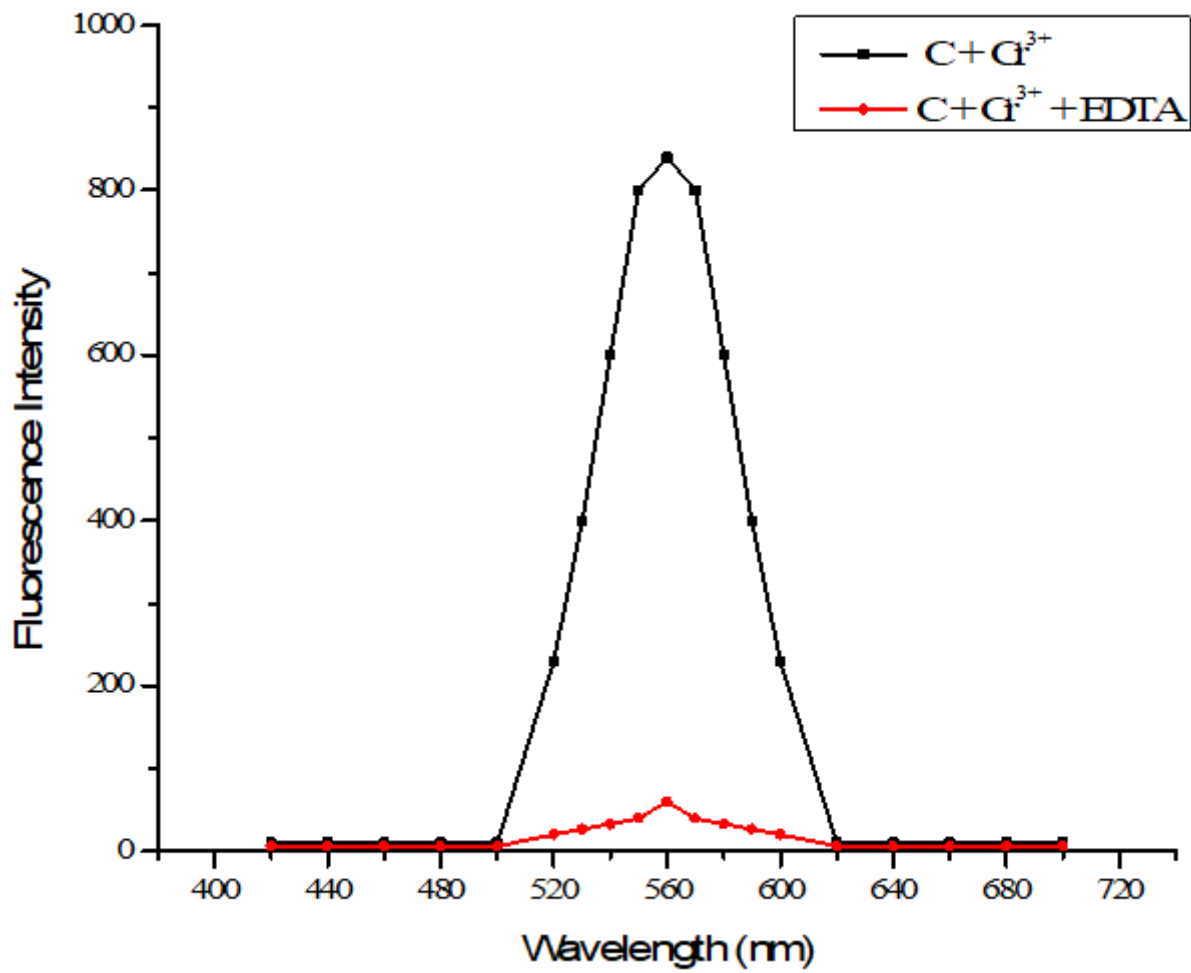


Figure 10

Reversibility experiment of sensor C complex with EDTA at λ_{em} 560 nm.

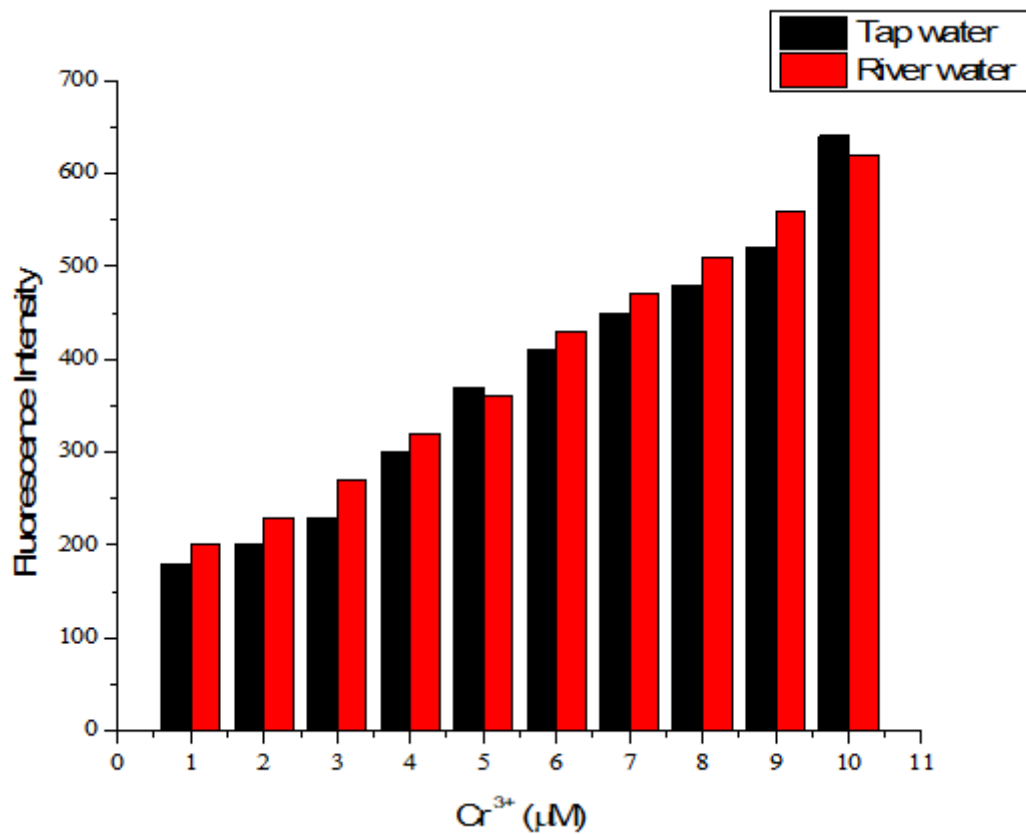


Figure 11

Detection of chromium in real watersamplesat560 nm.

Supplementary Files

This is a list of supplementary files associated with this preprint. Click to download.

- [GraphicalAbstract.png](#)
- [Scheme1.png](#)
- [Scheme2.png](#)